

## Article

# Targeted Isolation of Xenicane Diterpenoids From Taiwanese Soft Coral *Asterospicularia laurae*

Yu-Chi Lin <sup>1</sup>, Yi-Jen Chen <sup>2</sup>, Shu-Rong Chen <sup>3</sup>, Wan-Ju Lien <sup>4</sup>, Hsueh-Wei Chang <sup>4,5,6,7</sup>, Yu-Liang Yang <sup>1,3,8</sup>, Chia-Ching Liaw <sup>9,10</sup>, Jui-Hsin Su <sup>11</sup>, Ching-Yeu Chen <sup>12,\*</sup> and Yuan-Bin Cheng <sup>1,2,3,\*</sup>

- <sup>1</sup> Department of Marine Biotechnology and Resources, National Sun Yat-sen University, Kaohsiung 804351, Taiwan; m8952612@hotmail.com (Y.-C.L.); ylyang@gate.sinica.edu.tw (Y.-L.Y.)
- <sup>2</sup> Department of Fragrance and Cosmetic Science, College of Pharmacy, Kaohsiung Medical University, Kaohsiung 807378, Taiwan; mermaid190111@gmail.com
- <sup>3</sup> Graduate Institute of Natural Products, Center for Natural Product Research and Development, College of Pharmacy, Kaohsiung Medical University, Kaohsiung 807378, Taiwan; highshorter@hotmail.com
- <sup>4</sup> Department of Biomedical Science and Environmental Biology, PhD Program in Life Science, College of Life Science, Kaohsiung Medical University, Kaohsiung 80708, Taiwan; rfsl.lien@gmail.com (W.-J.L.); changhw@kmu.edu.tw (H.-W.C.)
- <sup>5</sup> Center for Cancer Research, Kaohsiung Medical University, Kaohsiung 80708, Taiwan
- <sup>6</sup> Cancer Center, Kaohsiung Medical University Hospital, Kaohsiung 80708, Taiwan
- <sup>7</sup> Department of Medical Research, Kaohsiung Medical University Hospital, Kaohsiung 80708, Taiwan
- <sup>8</sup> Agricultural Biotechnology Research Center, Academia Sinica, Taipei 115, Taiwan
- <sup>9</sup> Division of Chinese Materia Medica Development, National Research Institute of Chinese Medicine, Taipei 11221, Taiwan; liawcc@nricm.edu.tw
- <sup>10</sup> Department of Biochemical Science and Technology, National Chiayi University, Chiayi 60004, Taiwan
- <sup>11</sup> Graduate Institute of Marine Biology, National Dong Hwa University, Pingtung 944401, Taiwan; x2219@nmma.gov.tw
- <sup>12</sup> Department of Physical Therapy, Tzu-Hui Institute of Technology, Pingtung 92641, Taiwan
- \* Correspondence: chingyeu1971@yahoo.com.tw (C.-Y.C.); jmb@mail.nsysu.edu.tw (Y.-B.C.); Tel.: +886-8-779-9821-8639 (C.-Y.C.); +886-07-525-2000 (ext. 5212) (Y.-B.C.)



**Citation:** Lin, Y.-C.; Chen, Y.-J.; Chen, S.-R.; Lien, W.-J.; Chang, H.-W.; Yang, Y.-L.; Liaw, C.-C.; Su, J.-H.; Chen,

C.-Y.; Cheng, Y.-B. Targeted Isolation of Xenicane Diterpenoids From Taiwanese Soft Coral *Asterospicularia laurae*. *Mar. Drugs* **2021**, *19*, 123. <https://doi.org/10.3390/md19030123>

Academic Editor: Vassilios Roussis

Received: 3 February 2021

Accepted: 23 February 2021

Published: 25 February 2021

**Publisher's Note:** MDPI stays neutral with regard to jurisdictional claims in published maps and institutional affiliations.



**Copyright:** © 2021 by the authors. Licensee MDPI, Basel, Switzerland. This article is an open access article distributed under the terms and conditions of the Creative Commons Attribution (CC BY) license (<https://creativecommons.org/licenses/by/4.0/>).

**Abstract:** Application of LC-MS/MS-based molecular networking indicated the ethanol extract of octocoral *Asterospicularia laurae* is a potential source for the discovery of new xenicane derivatives. A natural product investigation of this soft coral resulted in the isolation of four new xenicane diterpenoids, asterolaurins O–R (1–4), together with six known compounds, xeniolide-A (5), isoxeniolide-A (6), xeniolide-B (7), 7,8-epoxyxeniolide-B (8), 7,8-oxido-isoxeniolide-A (9), and 9-hydroxyxeniolide-F (10). The structures of isolated compounds were characterized by employing spectroscopic analyses, including 2D-NMR (COSY, HMQC, HMBC, and NOESY) and high-resolution electrospray ionization mass spectrometry (HRESIMS). Asterolaurin O is the first case of brominated tricyclic type floridicin in the family Xenidiidae. Concerning bioactivity, the cytotoxic activity of those isolates was evaluated. As a result, compounds 1 and 2 demonstrated a selective cytotoxic effect against the MCF-7 cell line at IC<sub>50</sub> of 14.7 and 25.1 μM, respectively.

**Keywords:** *Asterospicularia laurae*; GNPS molecular networking; xenicane; cytotoxic

## 1. Introduction

Marine organisms such as sponges, soft corals, tunicates, and alga were regarded as plentiful sources of bioactive molecules, and many marine natural products or their derivatives have been used as drug candidates. Over the past 40 years, nearly 59% of antitumor agents have come from small-molecule natural products or inspired from natural sources [1]. So far, natural product investigations of *Asterospicularia* sp. resulted in a new pentahydroxylated sterol named 24ξ-Methyl-5α-cholestane-3β,5,6β,22R,24-pentol 6-acetate together with 14 new xenicane-type diterpenoids (13-*epi*-9-deacetoxyxenicin and asterolaurins A–M) [2–7]. Among those isolates, 13-*epi*-9-deacetoxyxenicin exhibited strong

cytotoxicity against P388D<sub>1</sub> mouse lymphoma cells with an IC<sub>50</sub> of 2.17 μM [3], asterolaurin A exhibited moderate cytotoxicity against HepG2 cells with an IC<sub>50</sub> of 8.9 μM, asterolaurin D showed inhibition of elastase release and superoxide anion generation with IC<sub>50</sub> values of 18.7 and 23.6 μM, respectively [4], asterolaurin L showed moderate cytotoxic activity against HEp-2, Daoy, MCF-7, and WiDr tumor cell lines, with ED<sub>50</sub> values of 11.8, 17.8, 11.7, and 17.4 μg/mL, respectively [5]. Moreover, 13-*epi*-9-desacetylxenicin, first isolated from *Xenia Novae-Britanniae*, also yielded from *A. laurae*, demonstrated significantly cytotoxic against Molt 4 (human T lymphoblast; acute lymphoblastic leukemia), K562 (human blood chronic myelogenous leukemia), Sup-T1 (Human T cell lymphoblastic lymphoma), and U937 (Human Caucasian histiocytic lymphoma) cells with IC<sub>50</sub> values of 1.30, 1.19, 3.17, 2.45 μM, respectively [7]. LC-MS/MS-based metabolite profiling has gradually become the mainstream of modern natural product investigation. This method provides a quick and visible spectrum for natural product de-replication [8,9] and targeted isolation [10]. As an assistant of this approach, *A. laurae*, collected in Orchid Island, Taiwan, were evaluated, and it demonstrated an abundance of xenicane-type diterpenes. As stated above, xenicane-type diterpenes could be potential sources of new antitumor agents; therefore, our continuing marine natural product investigation of bioactivity substances focuses on it. This article reports the isolation, structure determination, and bioactivity evaluation of the marine metabolites isolated from *A. laurae*.

## 2. Results and Discussion

The ethanol extract of *A. laurae* was partitioned between EtOAc and H<sub>2</sub>O to obtain an EtOAc-soluble layer. This layer was further partitioned between hexanes and 75% MeOH<sub>(aq)</sub> to remove the low polarity metabolites. The 75% MeOH layer was analyzed by the LC-MS/MS (negative ion mode). The MS/MS data were uploaded to the Global Natural Products Social Molecular Networking (GNPS, <https://gnps.ucsd.edu/> (accessed on 3 February 2021)) website, and the output data were mapped to create correlated clusters.

A cluster (Figure 1) with molecular weights of nodes between 276 and 384 was found to have the MS/MS fragment peaks of xenicane-type diterpenes (Figure S45), suggesting this group of metabolites could be xenicane-type diterpenes. A de-replication work was subsequently executed by comparing those molecular weights of nodes to known xenicanes. This investigation indicated that *A. laurae* should be a rich sources of new xenicane-type diterpenes.

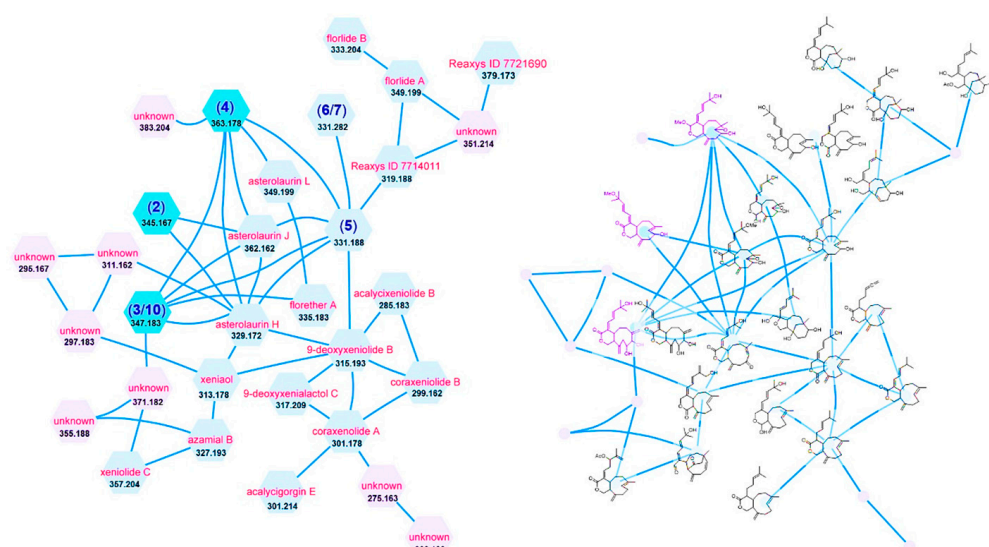


**Figure 1.** Cluster (left: molecular weight and proposed name; right: proposed chemical structure) of the xenicane-type diterpenes from the extract of *A. laurae*.

Four new compounds named asterolaurins O–R (1–4) along with six known xeniolide diterpenoids, xeniolide-A (5) [11], isoxeniolide-A (6) [12], xeniolide-B (7) [11], 7,8-epoxyxeniolide-B (8) [13], 7,8-oxido-isoxeniolide-A (9) [11], and 9-hydroxyxeniolide-F (10) [14] (Figure 2) were isolated and purified by successive silica gel, Sephadex LH-20, and semi-preparative normal-phase and reversed-phase high performance liquid chromatography (HPLC) columns. Their structures were further elucidated by spectroscopic data and compared with the relative literature.

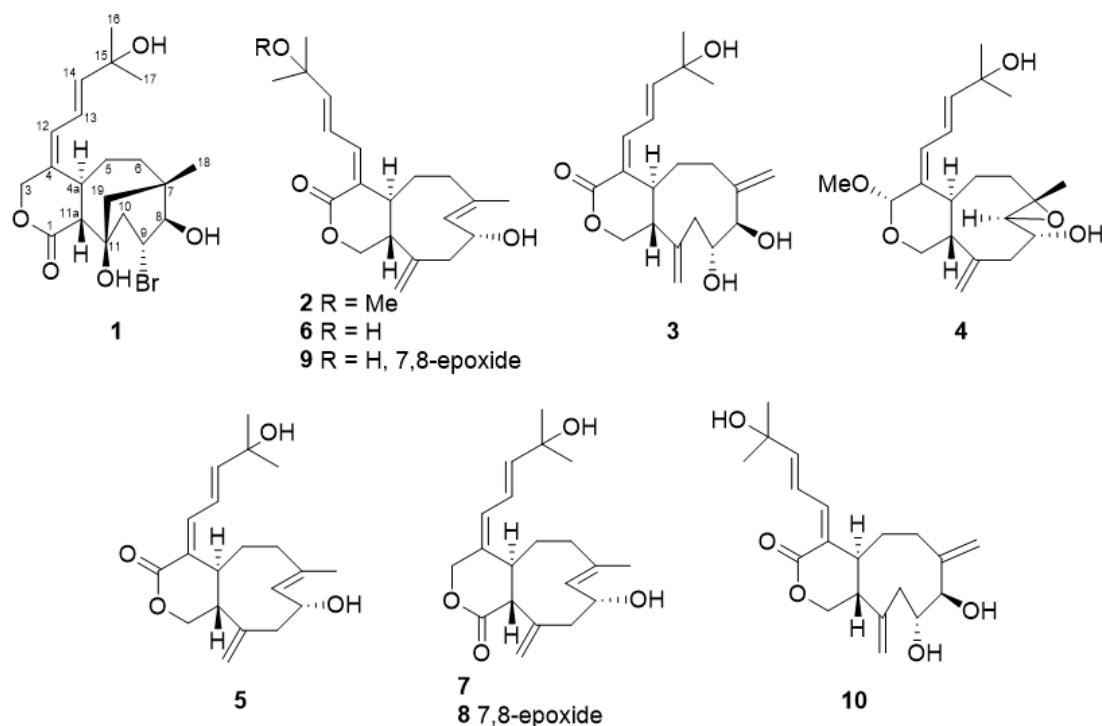


**Figure 2.** Structures of compounds 1–10 isolated from *A. laurae*.

Asterolaurin O (1) was obtained as an amorphous, colorless gum. The infrared (IR) data indicated the presence of hydroxy ( $3424\text{ cm}^{-1}$ ) and ester carbonyl ( $1719\text{ cm}^{-1}$ ) functionalities. The presence of one bromine atom in 1 was apparent from the isotopic pattern in a 1:1 ratio observed for the quasi-molecular ion peaks at  $451.11\text{ [M + Na]}^+$  and  $453.12\text{ [M + Na + 2]}^+$ , accompanied by an  $[\text{M} + \text{H}]^+$  fragment at  $m/z\ 429.04$  and  $431.11$ , and its molecular formula was assigned as  $\text{C}_{20}\text{H}_{29}\text{BrO}_5$  by high-resolution ESIMS ( $m/z\ 451.10903\text{ [M + Na]}^+$ , calculated for  $\text{C}_{20}\text{H}_{29}\text{BrNaO}_5$ ,  $451.10906$ ), implying 6 degrees of unsaturation. The  $^{13}\text{C}$  NMR and distortionless enhancement by polarization transfer (DEPT) spectra showed the presence of four olefinic carbons ( $\delta_{\text{C}}\ 122.3\text{ (d)}$ ,  $129.7\text{ (d)}$ ,  $137.0\text{ (c)}$ , and  $146.2\text{ (d)}$ ) and a lactone carbonyl  $\delta_{\text{C}}\ 176.9\text{ (s)}$ , suggesting that 1 was tricyclic. Detailed inspection of  $^1\text{H}$  and  $^{13}\text{C}$  NMR spectra of 1 (Table 1) disclosed signals characteristic for the A ring and the side chain were similar to those in florldide A [15], such as two singlet methyl protons ( $\delta_{\text{H}}\ 1.30 \times 2$ ) on a quaternary carbon ( $\delta_{\text{C}}\ 71.3$ , C-15) substituted by a hydroxyl group, were assigned to H-16 and H-17. Moreover, the diene resonance due to H-13 ( $\delta_{\text{H}}\ 6.34$ , dd,  $J = 11.1, 15.3\text{ Hz}$ ) was correspondingly coupled to H-12 ( $\delta_{\text{H}}\ 6.15$ , d,  $J = 11.1\text{ Hz}$ ) and H-14 ( $\delta_{\text{H}}\ 5.94$ , d,  $J = 15.3\text{ Hz}$ ). Additionally, the chemical shifts of diene protons combined with the appearance of lactone carbonyl signal, as well as an AB spin system oxymethylene at  $\delta_{\text{H}}\ 4.44\text{ (1H, d, } J = 12.0\text{ Hz)}$  and  $5.06\text{ (1H, br d, } J = 12.0\text{ Hz)}$  implied that 1 should belong to a xeniolide B type pyran-cyclononane diterpenoid. Analysis of the  $^1\text{H}$ - $^1\text{H}$  COSY and HMBC spectra (Figure 3) corroborated the plane structure of 1. COSY correlations between two de-shielded protons H-8 ( $\delta_{\text{H}}\ 4.09$ , d,  $5.7$ ;  $\delta_{\text{C}}\ 72.9$ ) and H-9 ( $\delta_{\text{H}}\ 4.37$ , td,  $5.7, 8.7$ ;  $\delta_{\text{C}}\ 75.1$ ), the latter one also correlating to H-10 ( $\delta_{\text{H}}\ 2.22$ , d,  $5.7$  and  $2.24$ , d,  $8.7$ ;  $\delta_{\text{C}}\ 39.8$ ), were observed. The other spin system for H-11a/H-4a/H-5/H-6 from the COSY spectrum as well as HMBC

correlations from Me-18 to C-6, C-7, C-8, and C-19, from isolated AB quartet protons H<sub>2</sub>-19 to C-7, C-11, and C-11a, from H-11a to C-1, C-11, and C-19 had established the bicyclic [4.3.1] ring system in **1**. Two hydroxyl groups were positioned at C-8 and C-11 due to some similar bicyclic [4.3.1] analogues being yielded from *Xenia* species, and possessed the same substitutes [15–19]. Thus, the residue bromine should be attached at the C-9 position to meet the data from NMR and mass, and the gross structure of **1** was identified. The relative stereochemistry of compound **1** was established from NOESY correlations (Figure 3) and by comparison of its spectroscopic data to those of xeniolide analogues. The *E* geometry of the Δ<sup>13</sup> double bond was established by the large coupling constant observed between H-13 and H-14 (*J* = 15.3 Hz). Furthermore, the geometry of the olefinic bond between C-4 and C-12 was concluded to be *E*, based on a strong NOESY correlation between H-4a (δ<sub>H</sub> 3.18) and H-13 was observed. The large coupling constant (*J* = 12.0 Hz) between H-4a and H-11a allowed us to assume H-4a was α-orientation, whereas H-11a was β-orientation. The NOESY correlations of H-19<sub>A</sub>/H-11a/H-19β/Me-18 revealed H<sub>2</sub>-19 and Me-18 were both on the β-side of **1**. Based on the above results, we could deduce that the stereochemistry of ring junctions (C-7 and C-11) in the bicyclic [4.3.1] scaffold of **1** were the same with those of floridicins [17]. The NOESY correlations of H-10α/H-4a/H-6α/H-8 revealed those protons were on the α-side of **1**. On the contrary, the NOESY correlations of H-6β/Me-18/H-19β/H-9/H-10β revealed that those protons were on the β-side of **1**. Therefore, the structure of **1** (asterolaurin O) was assigned as 9α-bromo-florlide A on the basis of the above results. This structure represents the first case of brominated tricyclic floridicin among the plethora of diterpenoid compounds already reported from corals.

**Table 1.** <sup>1</sup>H-NMR and <sup>13</sup>C-NMR data for compounds **1–4**.

	<b>1</b> <sup>b</sup>		<b>2</b> <sup>a</sup>		<b>3</b> <sup>b</sup>		<b>4</b> <sup>c</sup>	
	δ <sub>H</sub> ( <i>J</i> in Hz)	δ <sub>C</sub>	δ <sub>H</sub> ( <i>J</i> in Hz)	δ <sub>C</sub>	δ <sub>H</sub> ( <i>J</i> in Hz)	δ <sub>C</sub>	δ <sub>H</sub> ( <i>J</i> in Hz)	δ <sub>C</sub>
1		176.9, s	4.11, dd (5.9, 11.3) 3.63, t (11.3)	72.4, t	4.09, dd (4.1, 11.0) 3.91, t (11.0)	71.5, t	3.61, dd (6.5, 11.5) 3.28, t (11.5)	65.9, t
3	4.44, d (12.0) 5.06, d (12.0)	73.2, t		171.4, s		172.2, s	5.17, brs	99.2, d
4		137.0, s		134.6, s		133.3, s		138.5, s
4a	3.18, t (12.0)	39.3, d	2.70, dt (2.9, 11.0)	52.0, d	3.17, t (9.2)	42.8, d	2.97, brd (11.5)	43.1, d
5	1.95, m 1.87, m	33.4, t	1.61, m	39.1, t	1.84, m	38.5, t	1.61, m 1.83, m	34.8, t
6α	2.08, m	40.8, t	2.19, m	40.9, t	1.92, m	31.0, t	2.20, t (3.6)	40.5, t
6β	1.82, m						2.22, t (3.6)	
7		37.4, s		133.2, s		149.0, s		59.2, s
8	4.09, d (5.7)	71.2, d	5.26, d (7.4)	131.8, d	3.97, d (9.0)	83.1, d	3.00, d (8.0)	66.9, d
9	4.37, td (5.7, 8.7)	75.1, d	4.72, t (7.4)	67.9, d	4.06, dd (3.9, 9.0)	70.5, d	3.80, dd (8.0, 7.4)	69.1, d
10α	2.24, d (8.7)	39.8, t	2.34, d (13.6)	46.2, t	2.48, m	45.0, t	2.45, m	44.7, t
10β	2.22, d (5.7)		2.50, dd (13.6, 6.4)		2.60, m		2.47, t (7.4)	
11		72.5, s		149.5, s		148.3, s		147.4, s
11a	2.88, d (12.0)	57.3, d	2.06, dd (5.9, 11.0)	51.1, d	2.46, m	44.7, d	2.26, dd (6.5, 11.5)	50.7, d
12	6.15, d (11.1)	129.7, d	6.53, d (11.0)	137.3, d	7.04, d (11.8)	140.4, d	6.36, d (11.3)	126.5, d
13	6.34, dd (11.1, 15.3)	122.3, d	6.76, dd (11.0, 15.7)	126.6, d	6.57, dd (11.8, 15.1)	121.7, d	6.44, dd (11.3, 14.9)	120.4, d
14	5.94, d (15.3)	146.2, d	5.98, d (15.7)	146.4, d	6.35, d (15.1)	153.2, d	5.97, d (14.9)	144.6, d
15		71.3, s		76.5, s		71.5, s		71.0, s
16	1.30, s	29.8, q	1.30, s	26.0, q	1.34, s	29.7, q	1.32, s	29.9, q
17	1.30, s	29.8, q	1.30, s	25.9, q	1.34, s	29.7, q	1.32, s	29.9, q
18	1.15, s	34.7, q	1.70, s	17.3, q	5.20, d (1.6) 5.10, d (1.6)	120.2, t	1.44, s	17.3, q
19 <sub>A</sub>	1.76, d (14.6)	44.7, t	5.06, s	115.3, t	5.02, d (1.8)	116.5, t	4.85, s	114.8, t
19 <sub>B</sub>	1.84, d (14.6)		4.95, s		4.84, d (1.8)		5.11, s	
OH	4.61, brs							
OMe			3.16, s	50.9, q			3.47, s	55.1, q

<sup>a</sup> <sup>1</sup>H and <sup>13</sup>C-NMR were measured in MeOH-*d*<sub>4</sub> at 600 and 150 MHz, respectively. <sup>b</sup> <sup>1</sup>H and <sup>13</sup>C-NMR were measured in MeOH-*d*<sub>4</sub> at 700 and 175 MHz, respectively. <sup>c</sup> <sup>1</sup>H and <sup>13</sup>C-NMR were measured in CDCl<sub>3</sub> at 600 and 150 MHz, respectively.

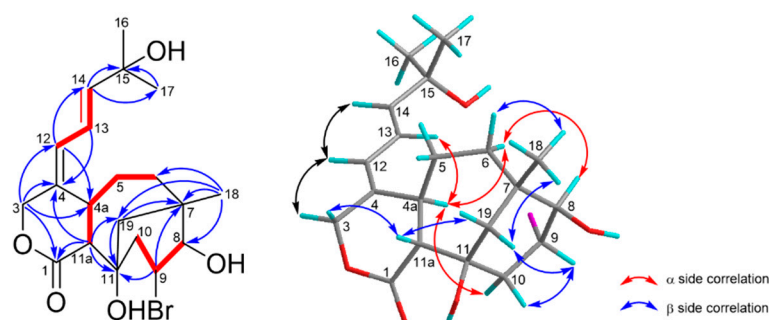


**Figure 3.** COSY (bold bond), selected HMBC (arrow), and NOESY (left-right arrow) correlations of **1**.

Asterolaurin P (**2**) was obtained as a pale yellowish amorphous gum with a molecular formula of  $C_{21}H_{30}O_4$  with 7 indices of hydrogen deficiency, as established based on its  $^{13}C$  NMR data and an HRESIMS pseudo-molecular ion peak at  $m/z$  369.20379  $[M + Na]^+$  (calcd for 369.20363). The IR spectrum indicated absorption bands due to hydroxyl ( $3454\text{ cm}^{-1}$ ) and ester carbonyl ( $1727\text{ cm}^{-1}$ ) functionalities, whereas the UV ( $\lambda_{\text{max}}$  237 and 215 nm) also supported a conjugated diene system. The structure of **1** was completely identified by a combination of 1D and 2D nuclear magnetic resonance experiments. The carbon resonances at  $\delta_C$  126.6 (CH), 131.8 (CH), 133.2 (qC), 134.6 (qC), 137.3 (CH), and 146.4 (CH) in the  $^{13}C$  NMR and DEPT spectra (Table 1) suggested the presence of three double bonds, and the quaternary carbon signal at  $\delta_C$  149.5 along with the methylene olefinic carbon signal at  $\delta_C$  115.3 indicated the presence of an *exo*-methylene double bond. Moreover, an ester  $\delta_C$  171.4 (qC) was also observed that implied that **2** was a bicyclic compound. The  $^1H$  NMR spectrum (Table 1) confirmed the presence of an *exo*-methylene double bond by two singlet signals at  $\delta_H$  4.95 and 5.06. Three spin systems (**I–III**, Figure 1) were deduced from combined  $^1H$ - $^1H$  COSY (Figure 4) and HSQC spectra of **1**. Fragment **I** consisted of a sequence of three double bond methines, and fragment **II** started from an oxymethylene ( $\delta_H$  3.63, 4.11) and ended with the relative deshielding methylene ( $\delta_H$  2.19) as well as fragment **III**, which included a carbinolic proton ( $\delta_H$  4.72;  $\delta_C$  67.9) and was correlated with the fourth double bond methine ( $\delta_H$  5.26;  $\delta_C$  131.8) and with allylic methylene ( $\delta_H$  2.34 and 2.50). These subunits were connected through key HMBC correlations (Figure 4) of H-1 ( $\delta_H$  3.63, 4.11) with C-3 ( $\delta_C$  171.4) and C-4a ( $\delta_C$  52.0), of H-12 ( $\delta_H$  6.53) with C-4a, of protons H-13 ( $\delta_H$  6.76), H-14 ( $\delta_H$  5.98), Me-16 ( $\delta_H$  1.30), and methoxy ( $\delta_H$  3.18) with C-15 ( $\delta_C$  76.5), of Me-18 ( $\delta_H$  1.70) with C-6 ( $\delta_C$  40.9), C-7 ( $\delta_C$  133.2), and C-8 ( $\delta_C$  131.8), as well as of exomethylene protons ( $\delta_H$  4.95, 5.06) with C-10 ( $\delta_C$  46.2), C-11 ( $\delta_C$  49.5), and C-11a ( $\delta_H$  51.1). Based on the above results, the gross structure of asterolaurin P could be constructed. The coupling constant ( $J = 11.0$  Hz) between H-4a and H-11a suggested a *trans* ring junction, which implied that H-4a was  $\alpha$ -oriented. The *Z* geometry of the  $\Delta^{4,12}$  double bond was deduced on the basis of the NOESY (Figure 4) cross-peaks H-12/H-4a, and the chemical shift of C-4a in **1** was shifted -9.8 ppm, compared with its  $\Delta^{4,12}$  *E* isomer, due to a  $\gamma$  effect of C-13 [7]. Additionally, the chemical shift of H-13 at  $\delta_H$  6.76, which is downfield-shifted to the corresponding *E* isomer ( $\delta_H$  6.40) due to an anisotropic effect, occurred with the carbonyl group. Moreover, the *E* geometry of the  $\Delta^{13}$  double bond was established by the large coupling constant observed between H-13 and H-14 ( $J = 15.7$  Hz). On the other hand, the  $\Delta^7$  double bond could be determined as an *E* configuration according to the  $^{13}C$  chemical shift of Me-18, which was 17.3 rather than at 22–25 for *Z* configuration [20]. The large coupling constant ( $J = 11.0$  Hz) between H-4a and H-11a suggested a *trans*-junction of the two rings, which implied that H-4a was  $\alpha$ -oriented. The NOESY correlations of H-4a with H-8, which presented quasi-axial on the  $\alpha$ -face, and on the other hand, of H-11a with Me-18, exhibited a quasi-axial on the  $\beta$ -face as well as Me-18 and also showed correlation with H-9 revealed an  $\alpha$ -orientation of the hydroxyl group at the C-9 position. Therefore, the structure of asterolaurin P was assigned as **2** based on the above results.

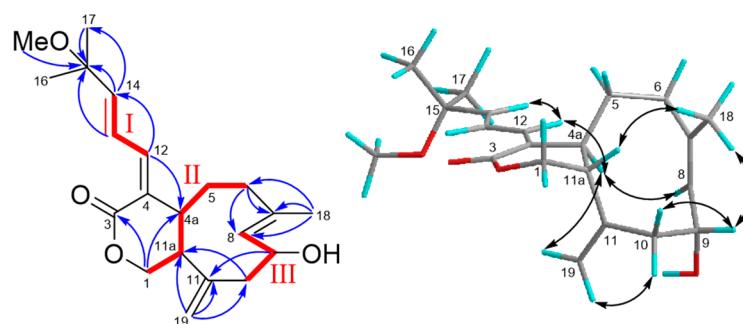


**Figure 4.** COSY (bold bond), selected HMBC (arrow), and NOESY (left-right arrow) correlations of **2**.

The molecular formula of  $C_{20}H_{28}O_5$  was deduced for asterolaurin Q (**3**) from its HRESIMS data, being consistent with 7 indices of hydrogen deficiency. The IR absorptions at  $3420$  and  $1704\text{ cm}^{-1}$  indicated the presence of hydroxy and ester carbonyl groups, respectively. The NMR spectral data of **3** revealed a ring A similar to those of **1** because of an AB system of  $H_2-1$  at  $\delta_H$  4.09 (dd, 4.1, 11.0) and 3.91 (d, 11.0 Hz) was observed. The diene system, H-13 at  $\delta_H$  6.57 (dd,  $J = 11.8, 15.1$  Hz), was coupled to H-12 ( $\delta_H$  7.04, d,  $J = 11.8$  Hz) and H-14 ( $\delta_H$  6.35, d,  $J = 15.1$  Hz), whereas the downfield shift of H-12 attributed to an anisotropy effect occurred with carbonyl group at C-3 that implied the *E* form configuration of  $\Delta^{4,12}$  double bond in **3**. In the aided DEPT spectra,  $^{13}C$  NMR resonances at  $\delta_C$  116.5 ( $CH_2$ ) and 120.1 ( $CH_2$ ) indicated the presence of two exo methylene double bonds, which were confirmed by the observation of four doublet signals at  $\delta_H$  4.84 (d, 1.8), 5.02 (d, 1.8), 5.10 (d, 1.6), and 5.20 (d, 1.6) in the  $^1H$  NMR spectrum. Besides, the presence of two oxygenated methines was deduced from the carbon signal at  $\delta_C$  83.1 and 70.5, corresponded to the proton signal at  $\delta_H$  3.97 (d, 9.0) and 4.06 (dd, 3.9, 9.0), respectively. The COSY spectrum (Figure 5) showed cross-peaks with signals at H-12/H-13/H-14; H-1 ( $\delta_H$  4.09, 3.91)/H-11a ( $\delta_H$  2.46, m)/H-4a ( $\delta_H$  3.17)/H-5 ( $\delta_H$  1.84, m)/H-6 ( $\delta_H$  1.92, m); H-8 ( $\delta_H$  3.97)/H-9 ( $\delta_H$  4.06)/H-10 ( $\delta_H$  2.48, 2.60). Furthermore, the key HMBC correlations (Figure 5) of both H-1 and H-12 with C-3 ( $\delta_C$  171.4) and C-4a ( $\delta_C$  52.0), as well as H-13, H-14, Me-16 and Me-17 with C-15 ( $\delta_C$  76.5), allowed a  $\delta$ -valerolactone ring linked with (via C-4) a diene which extended to an oxyquaternary carbon bearing two geminal methyls in **2**. The HMBC correlations of H-6 with C-8, of H-10 with C-11a, of exomethylene protons ( $\delta_H$  5.10, 5.20, H-18) with C-6 and C-8, and of exomethylene protons ( $\delta_H$  5.02, 4.84, H-19) with C-10 and C-11a, allowed the construction of a cyclononane ring with two exomethylene functionalities at C-7 and C-11. Considering the molecular formula of **3** as well as the chemical shifts of C-8 ( $\delta_C$  83.1), C-9 ( $\delta_C$  70.5), and C-15 ( $\delta_C$  71.5), three hydroxy groups were attached at the abovementioned positions. Herein, the gross structure of **3** was assigned. The *trans* junction of the two rings was suggested by coupling constant ( $J = 9.2$  Hz) between H-4a and H-11a, and the configuration of H-4a could be assumed as  $\alpha$ -oriented. Additionally, the NOESY correlations (Figure 4) of H-19/H-4a/H-13 and also the correlations of H-5 $\alpha$ /H-13/H-6 $\alpha$ /H-18/H-8 revealed those protons were on the same  $\alpha$  face of the structure. On the other hand, the NOESY cross-peaks of H-11a/H-5 $\beta$ /H-9 implied that H-9 was  $\beta$ -orientation. Therefore, the structure of asterolaurin P was assigned as **3** on the basis of the above results.

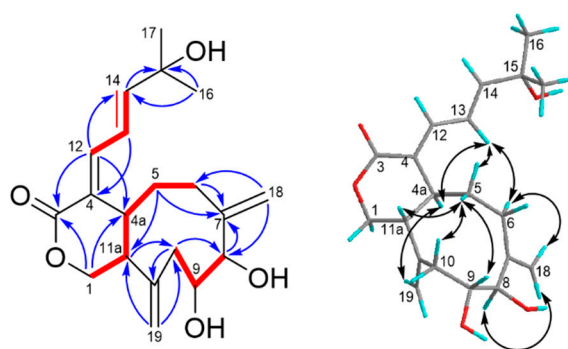


**Figure 5.** COSY (bold bond), selected HMBC (arrow), and NOESY (left-right arrow) correlations of **3**.

Compound **4** was isolated as an amorphous gum, and its molecular formula was established as  $C_{21}H_{32}O_5$  by HREIMS and NMR spectral data. The  $^1H$  and  $^{13}C$  NMR spectra of **4** showed some characteristic signals in the cyclononane skeleton as B ring moiety, similar to those of compounds **8** and **9**. Two singlets at  $\delta_H$  5.11 and 4.85 corresponding to  $\delta_C$  144.8 were typical of resonances due to exocyclic methylene protons at C-19. A methyl-bearing *E* trisubstituted epoxide [ $\delta_H$  1.43 s, 3.00 (d, 8.0);  $\delta_C$  17.3 q, 59.2 s, 66.9 d], and epoxide proton (H-8) was further shown, and coupled with oxymethine [ $\delta_H$  3.80, dd (8.0, 7.4),  $\delta_C$  69.1] it implied a hydroxy group attached at the C-9 position. Moreover, bands for a diene olefinic system at  $\delta_H$  6.36 (d, 11.3, H-12), 6.44 (dd, 14.9, 11.3, H-13), and 5.84 (d, 14.9, H-14) were also observed. COSY and HMBC correlations (Figure 6) supported the structure in which three spin fragments were connected in the aid of key HMBC corrections of Me-18 with C-6, C-7, and C-8, of H-19 with C-10, C-11, and C-11a, of an acetal proton H-3 ( $\delta_H$  5.17, brs;  $\delta_C$  99.2) with C-1, C-4, C-12, and methoxyl carbon ( $\delta_C$  55.1). Therefore, the structure of **4** could be established unambiguously. The 4(12) *E*-configuration and the *E*-geometry for  $\Delta^{13}$  double bonds were determined by NOESY correlation (Figure 6) between H-13 and H-4a, and the coupling constant between H-13 and H-14 (14.9), respectively. Ring junction proton H-4a was assumed as an  $\alpha$ -orientation, and H-11a was  $\beta$ -orientation due to the coupling constant between these two protons. On the  $\beta$ -face, H-11a showed the NOESY cross peak with Me-18, in turn coupled with H-9 revealed an  $\alpha$ -orientation of hydroxyl group at the C-9 position. Besides, NOESY correlations of H-19<sub>A</sub>/H-4a/H-8 unveiled  $\alpha$ -orientation of H-8. Based on the above results, we could infer that Me-18 was a  $\beta$ -quasi-axial orientation, whereas H-7 and H<sub>2</sub>-19 were  $\alpha$ -quasi-axial orientations. Thus, the relative stereochemistry of the cyclononane ring system was similar to that of asterolaurin A [4]. Additionally, the NOESY correlations of H-3 with H<sub>2</sub>-5 showed  $\beta$ -quasi-axial orientation revealed  $\alpha$ -orientation of methoxyl group at C-3 position. Thus the structure of asterolaurin R was unambiguously established as shown in Figure 6.

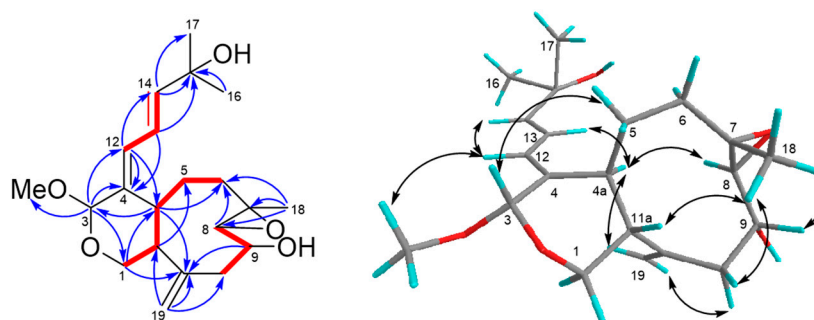


**Figure 6.** COSY (bold bond), selected HMBC (arrow), and NOESY (left-right arrow) correlations of **4**.

The cytotoxicities of all isolated marine natural products (**1–10**) were evaluated *in vitro* against human breast (MCF-7), oral (Ca9-22), and ovarian (SK-OV-3) carcinomas. As illustrated in Table 2, compounds **1** ( $IC_{50}$  = 14.7  $\mu$ M) and **2** ( $IC_{50}$  = 25.1  $\mu$ M) selectively

possessed strong activities against the MCF-7 cell. For the ovarian and oral cancer cells, all tested xenicane diterpenoids were inactive (>100  $\mu\text{M}$ ).

**Table 2.** Results of Cytotoxicities ( $\text{IC}_{50}$ ,  $\mu\text{M}$ ) of isolated compounds 1–10.

Compound/Tumor Cells	MCF-7	Ca9-22	SK-OV-3
1	14.7 $\pm$ 0.23	>100	>100
2	25.1 $\pm$ 4.1	>100	>100
3	>100	>100	>100
4	>100	>100	>100
5	>100	>100	>100
6	>100	>100	>100
7	>100	>100	>100
8	>100	>100	>100
9	>100	>100	>100
10	>100	>100	>100
Cisplatin <sup>a</sup>	19.8		13.8

<sup>a</sup> Positive control; data come from literatures [21,22].

### 3. Experimental

#### 3.1. General

Optical rotations were determined using a JASCO P-2100 polarimeter (Jasco, Tokyo, Japan), and IR spectra were recorded on a JASCO FT/IR-4600 infrared spectrometer (Jasco, Tokyo, Japan). NMR spectra were recorded on Varian 600 MHz NMR (Varian, Palo Alto, CA, USA) and Bruker AVIII-HD700X 700 MHz spectrometers (Bruker, Bremen, Germany). HRESIMS data were recorded on a VG Biotech Quattro 5022 mass spectrometer (VG Biotech, Altrincham, UK). GNPS data were obtained on an Agilent 6545XT AdvanceBio LC/Q-TOF mass spectrometer (Agilent Technologies, Santa Clara, CA, USA). Silica gel 60 (0.063–0.200 mm) was used for flash-column and open column chromatography (Merck KGaA, Darmstadt, Germany). Gel filtration column chromatography was performed with Sephadex LH-20 (GE Healthcare, Chicago, IL, USA). Precoated aluminum TLC plate/TLC silica gel 60 F<sub>254</sub> were used for TLC analysis (Merck KGaA, Darmstadt, Germany). Normal-phase semi-preparative HPLC was accomplished using a Luna Silica (5  $\mu\text{m}$ , 250  $\times$  10 mm) column (Phenomenex, Torrance, CA, USA) on an L-6000 pump with an L-4000 UV detector (Hitachi, Tokyo, Japan), while reversed-phase HPLC was using Luna CN or Biphenyl (5  $\mu\text{m}$ , 250  $\times$  10 mm) columns (Phenomenex, Torrance, CA, USA) on a Chromaster 5110 pump with a Chromaster 5410 UV detector (Hitachi, Tokyo, Japan).

#### 3.2. Animal Material

Specimens of soft coral *Asterospicularia laurae* were donated by Prof. Ya-Ching Shen in 2019. The animal materials were collected in August 2012 off the coast of Orchid Island, Taiwan. The samples were stored in a freezer until extraction. The material was identified by Prof. Dr. Jui-Hsin Su. A voucher sample (specimen code: AL001) was deposited at Department of Marine Biotechnology and Resources, National Sun Yat-sen University, Kaohsiung, Taiwan.

#### 3.3. Global Natural Product Social Molecular Networking

Equal divisions (10  $\mu\text{L}$ ) of the MeOH-layer of Taiwanese soft coral *A. laurae* were dispensed into 96-well plates, dried under nitrogen, and resuspended in DMSO (10  $\mu\text{L}$ ), and 10  $\mu\text{L}$  of a DMSO aliquot was injected into an Agilent 6545XT AdvanceBio LC/Q-TOF (quadrupole time-of-flight) equipped with an Agilent 1290 Infinity II LC system, eluting with an ACQUITY UPLC BEH C<sub>18</sub> column (1.7  $\mu\text{m}$ , 2.1  $\times$  100 mm, flow rate: 0.4 mL/min, Waters). The elution program, using water (A) and acetonitrile (B), both with 0.1% formic acid as mobile phases, started with a 5% isocratic elution for 1 min and was then followed by a linear gradient from 5% to 99.5% B until 16 min, and then maintained 99.5% B as a solvent system for 10 min followed by re-equilibration period for 2 min before the next

injection. The UPLC-Q-TOF(-)MS/MS data acquired for all samples at a fixed collision energy of 40 eV were converted from RAW data files to mzXML file format using the ProteoWizard MSconvert software [23] and uploaded to the Global Natural Products Social Molecular Networking Web server to create a molecular network [24]. The resulting spectral networks were imported into Cytoscape version 3.8.2 [25]. Careful review of these GNPS data associated with the Comprehensive Marine Natural Products Database and Reaxys® database highlighted a promising cluster (Figure 1 and Figure S45), as a possible source of new xenicane diterpenoids.

### 3.4. Extraction and Isolation

Soft coral *Asterospicularia laurae* (115.4 g, wet weight) was macerated with 95% ethanol (1.5 L, 3 times) at room temperature. The solvent was decanted and the extract was concentrated under reduced pressure to obtain a crude extract (31.4 g), which was partitioned between H<sub>2</sub>O and ethyl acetate to yield an ethyl acetate layer. The EtOAc layer was subsequently partitioned (hexanes/MeOH/H<sub>2</sub>O = 4:3:1) to obtain hexanes and MeOH layers. After <sup>1</sup>H NMR, experiments were co-referred with TLC assay as well as GNPS MS/MS analysis on all obtained layers, and the MeOH layer was selected for further isolation. The MeOH layer (5.2 g) was chromatographed by a normal-phase silica gel flash column eluted with a gradient solvent system of hexanes and ethyl acetate (5:1~0:1) followed by stepwise ethyl acetate with methanol (20:1~0:1) to obtain six subfractions (LA1~6), according to TLC analysis. The third sub-fraction, LA3, was fractionated over Sephadex LH-20 using MeOH and CH<sub>2</sub>Cl<sub>2</sub> (1:1) as a solvent to afford six subfractions (LA3-1~6). Fraction LA-3-5 was purified by normal-phase HPLC (hexane/dichloromethane/methanol, 50:45:5) to yield compounds **1** (2.7 mg), **3** (1.4 mg), **9** (1.6 mg), and **10** (2.3 mg). Fraction LA-3-4 was subjected to silica gel CC (CH<sub>2</sub>Cl<sub>2</sub>/MeOH, 1:0→0:1) to get five subfractions (LA3-4-1~5), and subfraction LA3-4-4 was further separated by normal-phase HPLC (hexane/dichloromethane/methanol, 57:38:5) to afford compounds **4** (1.4 mg), **7** (1.3 mg), and **8** (2.1 mg). Besides, Fr. LA3-4-3 was isolated by reverse-phase HPLC using a CN column and gave compound **2** (1.7 mg) along with two subfractions Fr. LA-3-4-3-1~2. The fraction LA-3-4-3-1 was isolated by RP-Biphenyl HPLC (methanol/H<sub>2</sub>O, 60/40) to give compounds **5** (0.5 mg) and **6** (0.5 mg).

### 3.5. Spectroscopic Data

Asterolaurin O (**1**) amorphous, colorless gum,  $[\alpha]_D^{26} -1.0^\circ$  (*c* 0.05, MeOH); IR (neat)  $\nu_{\max}$  3424, 2960, 2929, 1719, 1379, 1261, 1167, 1033 cm<sup>-1</sup>; <sup>1</sup>H-NMR and <sup>13</sup>C-NMR (CD<sub>3</sub>OD, 700/175 MHz) see Table 1; HRESIMS *m/z* 451.10903 (calcd for C<sub>20</sub>H<sub>29</sub>BrNaO<sub>5</sub>, 451.10906).

Asterolaurin P (**2**) pale yellowish amorphous gum,  $[\alpha]_D^{26} -47.6^\circ$  (*c* 0.05, MeOH); IR (neat)  $\nu_{\max}$  3454, 2926, 1727, 1455, 1263, 1029 cm<sup>-1</sup>; <sup>1</sup>H-NMR and <sup>13</sup>C-NMR (CD<sub>3</sub>OD, 600/150 MHz) see Table 1; HRESIMS *m/z* 369.20379 (calcd for C<sub>21</sub>H<sub>30</sub>O<sub>4</sub>Na, 369.20363).

Asterolaurin Q (**3**) amorphous, colorless gum,  $[\alpha]_D^{26} -1.0^\circ$  (*c* 0.05, MeOH); IR (neat)  $\nu_{\max}$  3420, 2962, 2927, 2360, 1703, 1638, 1261, 1091 cm<sup>-1</sup>; <sup>1</sup>H-NMR and <sup>13</sup>C-NMR (CD<sub>3</sub>OD, 700/175 MHz) see Table 1; HRESIMS *m/z* 371.18294 (calcd for C<sub>20</sub>H<sub>28</sub>O<sub>5</sub>Na, 371.18290).

Asterolaurin R (**4**) amorphous, colorless gum,  $[\alpha]_D^{26} -47.6^\circ$  (*c* 0.05, MeOH); IR (neat)  $\nu_{\max}$  3433, 2964, 1643, 1260, 1072 cm<sup>-1</sup>; <sup>1</sup>H-NMR and <sup>13</sup>C-NMR (CDCl<sub>3</sub>, 600/150 MHz) see Table 1; HRESIMS *m/z* 387.21425 (calcd for C<sub>21</sub>H<sub>32</sub>O<sub>5</sub>Na, 387.21420).

### 3.6. Cytotoxic Assays

Breast (MCF-7), oral (Ca9-22), and ovarian (SK-OV-3) cancer cell lines were available from the American Type Culture Collection (ATCC, Manassas, VA, USA) or the Japanese Collection of Research Bioresources (JCRB) Cell Bank (National Institute of Biomedical Innovation, Osaka, Japan). The cell viability was detected by MTS assay at 72 h treatment as previously described [24].

#### 4. Conclusions

With the assistance of molecular networking-based de-replication strategy, xenicane diterpenes were targeted and obtained from the marine soft coral *A. laurae*. Among ten isolated compounds, asterolaurins O–Q (1–3) were identified as new xeniolides (possessing a  $\delta$ -lactone-cyclononane skeleton), and asterolaurin R (4) was a new xenicin (containing an 11-oxabicyclo[7.4.0]tridecane ring system with an acetal functionality). It is noteworthy that asterolaurin O (1) was the first case of natural brominated tricarbocyclic floridicins yielded from the family Xeniiidae. Moreover, compared with other asterolaurins obtained from the genus *Asterospicularia*, asterolaurin O (1) showed potent inhibition toward MCF-7 cells. This finding suggests that brominated xenicane-type diterpenes were worthy for further cytotoxic evaluations.

**Supplementary Materials:** The HRESIMS, IR spectra,  $^1\text{H}$ ,  $^{13}\text{C}$ , DEPT, HSQC, COSY, HMBC, and NOESY spectra of compounds 1–4 are available online at <https://www.mdpi.com/1660-3397/19/3/123/s1>, Figure S1. The HRESIMS of asterolaurin O (1); Figure S2. The IR spectrum of asterolaurin O (1); Figure S3. The  $^1\text{H}$ -NMR spectrum of asterolaurin O (1) (700 MHz in  $\text{CD}_3\text{OD}$ ); Figure S4. The  $^1\text{H}$ -NMR spectrum (0.5–2.5 ppm) of asterolaurin O; Figure S5. The  $^{13}\text{C}$ -NMR spectrum of asterolaurin O (1) (175 MHz in  $\text{CD}_3\text{OD}$ ); Figure S6. The  $^{13}\text{C}$ -NMR spectrum (20–55 ppm) of asterolaurin O (1); Figure S7. The DEPT spectrum of asterolaurin O (1); Figure S8. The  $^1\text{H}$ - $^1\text{H}$  COSY spectrum of asterolaurin O (1); Figure S9. The HSQC spectrum of asterolaurin O (1); Figure S10. The HMBC spectrum of asterolaurin O (1); Figure S11. The NOESY spectrum of asterolaurin O (1); Figure S12. The HRESIMS of asterolaurin P (2); Figure S13. The IR spectrum of asterolaurin P (2); Figure S14. The  $^1\text{H}$ -NMR spectrum of asterolaurin P (2) (600 MHz in  $\text{CD}_3\text{OD}$ ); Figure S15. The  $^1\text{H}$ -NMR spectrum (0.5–2.5 ppm) of asterolaurin P; Figure S16. The  $^{13}\text{C}$ -NMR spectrum of asterolaurin P (2) (150 MHz in  $\text{CD}_3\text{OD}$ ); Figure S17. The  $^{13}\text{C}$ -NMR spectrum (15–55 ppm) of asterolaurin P (2); Figure S18. The DEPT spectra of asterolaurin P (2); Figure S19. The  $^1\text{H}$ - $^1\text{H}$  COSY spectrum of asterolaurin P (2); Figure S20. The HSQC spectrum of asterolaurin P (2); Figure S21. The HMBC spectrum of asterolaurin P (2); Figure S22. The NOESY spectrum of asterolaurin P (2); Figure S23. The HRESIMS of asterolaurin Q (3); Figure S24. The IR spectrum of asterolaurin Q (3); Figure S25. The  $^1\text{H}$ -NMR spectrum of asterolaurin Q (3) (700 MHz in  $\text{CD}_3\text{OD}$ ); Figure S26. The  $^1\text{H}$ -NMR spectrum (0.5–2.5 ppm) of asterolaurin Q; Figure S27. The  $^{13}\text{C}$ -NMR spectrum of asterolaurin Q (3) (175 MHz in  $\text{CD}_3\text{OD}$ ); Figure S28. The  $^{13}\text{C}$ -NMR spectrum (20–55 ppm) of asterolaurin Q; Figure S29. The DEPT spectrum of asterolaurin Q (3); Figure S30. The  $^1\text{H}$ - $^1\text{H}$  COSY spectrum of asterolaurin Q (3); Figure S31. The HSQC spectrum of asterolaurin Q (3); Figure S32. The HMBC spectrum of asterolaurin Q (3); Figure S33. The NOESY spectrum of asterolaurin Q (3); Figure S34. The HRESIMS of asterolaurin R (4); Figure S35. The IR spectrum of asterolaurin R (4); Figure S36. The  $^1\text{H}$ -NMR spectrum of asterolaurin R (4) (600 MHz in  $\text{CDCl}_3$ ); Figure S37. The  $^1\text{H}$ -NMR spectrum (0.5–2.5 ppm) of asterolaurin R; Figure S38. The  $^{13}\text{C}$ -NMR spectrum of asterolaurin R (4) (150 MHz in  $\text{CDCl}_3$ ); Figure S39. The  $^{13}\text{C}$ -NMR spectrum (15–55 ppm) of asterolaurin R; Figure S40. The DEPT spectra of asterolaurin R; Figure S41. The  $^1\text{H}$ - $^1\text{H}$  COSY spectrum of asterolaurin R (4); Figure S42. The HSQC spectrum of asterolaurin R (4); Figure S43. The HMBC spectrum of asterolaurin R (4); Figure S44. The NOESY spectrum of asterolaurin R (4); Figure S45. Negative Q-TOF MS/MS spectrum of xeniolide-A (5).

**Author Contributions:** Conceptualization, Y.-B.C. and C.-Y.C.; validation, S.-R.C.; investigation, Y.-C.L., Y.-J.C., W.-J.L. and H.-W.C.; resources, Y.-L.Y., C.-C.L. and J.-H.S.; writing—original draft preparation, Y.-C.L.; writing—review and editing, Y.-B.C. and S.-R.C.; funding acquisition, Y.-B.C. and C.-Y.C. All authors have read and agreed to the published version of the manuscript.

**Funding:** This research was funded by the Ministry of Science and Technology of Taiwan (MOST 108-2320-B-110-009-MY3).

**Institutional Review Board Statement:** Not applicable.

**Data Availability Statement:** Data are contained within the article and Supplementary Material.

**Conflicts of Interest:** The authors declare no conflict of interest.

## References

1. Newman, D.J.; Cragg, G.M. Natural products as sources of new drugs over the nearly four decades from 01/1981 to 09/2019. *J. Nat. Prod.* **2020**, *83*, 770–803. [[CrossRef](#)]
2. Ksebati, M.B.; Schmitz, F.J. 24 $\xi$ -Methyl-5 $\alpha$ -cholestane-3 $\beta$ ,5,6 $\beta$ ,22R,24-pentol 6-acetate: New polyhydroxylated sterol from the soft coral *Asterospicularia randalli*. *Steroids* **1984**, *43*, 639–649. [[CrossRef](#)]
3. Bowden, B.; Cusack, B.; Dangel, A. 13-Epi-9-deacetoxyxenicin, a cytotoxic diterpene from the Soft Coral *Asterospicularia laurae* (Alcyonacea). *Mar. Drugs* **2003**, *1*, 18–26. [[CrossRef](#)]
4. Lin, Y.-C.; El-Razek, M.H.A.; Hwang, T.-L.; Chiang, M.Y.; Kuo, Y.-H.; Dai, C.-F.; Shen, Y.-C. Asterolaurins A–F, xenicane diterpenoids from the Taiwanese soft coral *Asterospicularia laurae*. *J. Nat. Prod.* **2009**, *72*, 1911–1916. [[CrossRef](#)] [[PubMed](#)]
5. Lin, Y.-S.; Fazary, A.E.; Chen, C.-H.; Kuo, Y.-H.; Shen, Y.-C.; Asterolaurins, G.-J. New xenicane diterpenoids from the Taiwanese soft coral *Asterospicularia laurae*. *Helv. Chim. Acta* **2011**, *94*, 273–281. [[CrossRef](#)]
6. Lin, Y.-S.; Fazary, A.E.; Chen, C.-H.; Kuo, Y.-H.; Shen, Y.-C. Bioactive xenicane diterpenoids from the Taiwanese soft coral *Asterospicularia laurae*. *Chem. Biodiv.* **2011**, *8*, 1310–1317. [[CrossRef](#)]
7. Su, J.-H.; Liu, C.-I.; Lu, M.-C.; Chang, C.-I.; Hsieh, M.-Y.; Lin, Y.-C.; Dai, C.-F.; Zhang, Y.-H.; Lin, Z.-Y.; Lin, Y.-S. New secondary metabolite with cytotoxicity from spawning soft coral *Asterospicularia laurae* in Taiwan. *Nat. Prod. Res.* **2019**, 1–9. [[CrossRef](#)]
8. Watrous, J.; Roach, P.; Alexandrov, T.; Heath, B.S.; Yang, J.Y.; Kersten, R.D.; van der Voort, M.; Pogliano, K.; Gross, H.; Raaijmakers, J.M.; et al. Mass spectral molecular networking of living microbial colonies. *Proc. Natl. Acad. Sci. USA* **2012**, *109*, 1743–1752. [[CrossRef](#)]
9. Allard, P.-M.; Péresse, T.; Bisson, J.; Gindro, K.; Marcourt, L.; Pham, V.C.; Roussi, F.; Litaudon, M.; Wolfender, J.-L. Integration of molecular networking and in-silico ms/ms fragmentation for natural products de-replication. *Anal. Chem.* **2016**, *88*, 3317–3323. [[CrossRef](#)]
10. Chao, R.; Hou, X.-M.; Xu, W.-F.; Hai, Y.; Wei, M.-Y.; Wang, C.-Y.; Gu, Y.-C.; Shao, C.-L. Targeted Isolation of Asperheptatides from a Coral-Derived Fungus Using LC-MS/MS-Based Molecular Networking and Antitubercular Activities of Modified Cinnamate Derivatives. *J. Nat. Prod.* **2021**, *84*, 11–19. [[CrossRef](#)]
11. Kashman, Y.; Groweiss, A. Xeniolide-A and xeniolide-B, two new diterpenoids from the soft-coral *xenia macrospiculata*. *Tetrahedron Lett.* **1978**, *48*, 4833–4836. [[CrossRef](#)]
12. Braekman, J.C.; Daloz, D.; Tursch, B.; Declercq, J.P.; Germain, G.; Meerse, M.V. Chemical Studies of Marine Invertebrates. XXXIX. Three novel diterpenoids from the soft coral *Xenia novae-britanniae*. *Bull. Soc. Chim. Belg.* **1979**, *88*, 71–77. [[CrossRef](#)]
13. Kashman, Y.; Groweiss, A. New diterpenoids from the soft corals *Xenia macrospiculata* and *Xenia obscuronata*. *J. Org. Chem.* **1980**, *45*, 3814–3824. [[CrossRef](#)]
14. Anta, C.; González, N.; Santafé, G.; Rodríguez, J.; Jiménez, C. New xenia diterpenoids from the Indonesian soft coral *Xenia* sp. *J. Nat. Prod.* **2002**, *65*, 766–768. [[CrossRef](#)] [[PubMed](#)]
15. Iwagawa, T.; Kawasaki, J.-I.; Hase, T. New xenia diterpenes isolated from the soft coral, *Xenia florida*. *J. Nat. Prod.* **1998**, *61*, 1513–1515. [[CrossRef](#)]
16. Iwagawa, T.; Kawasaki, J.-I.; Hase, T.; Wright, J.L. New di- and tricyclic diterpenes possessing a bicyclic [4.3.1] ring system isolated from the soft coral, *Xenia florida*. *Tetrahedron* **1997**, *53*, 6809–6816. [[CrossRef](#)]
17. Iwagawa, T.; Kawasaki, J.-I.; Hase, T.; Yu, C.-M.; Walter, J.A.; Wright, J.L.C. A new tricyclic diterpene structure from the soft coral *Xenia florida*. *J. Chem. Soc. Chem. Com.* **1994**, 2073–2074. [[CrossRef](#)]
18. El-Gamal, A.A.H.; Chiang, C.-Y.; Huang, S.-H.; Wang, S.-K.; Duh, C.-Y. Xenia diterpenoids from the formosan soft coral *Xenia blumi*. *J. Nat. Prod.* **2005**, *68*, 1336–1340. [[CrossRef](#)]
19. El-Gamal, A.A.H.; Wang, S.-K.; Duh, C.-Y. Cytotoxic xenia diterpenoids from the soft coral *Xenia umbellata*. *J. Nat. Prod.* **2006**, *69*, 338–341. [[CrossRef](#)]
20. Couperus, P.A.; Clague, A.D.H.; Van Dongen, J.P.C.M. <sup>13</sup>C chemical shifts of some model olefins. *Org. Mag. Reson.* **1976**, *8*, 426–431. [[CrossRef](#)]
21. Ou-Yang, F.; Tsai, I.-H.; Tang, J.-Y.; Yen, C.-Y.; Cheng, Y.-B.; Farooqi, A.A.; Chen, S.-R.; Yu, S.-Y.; Kao, J.-K.; Chang, H.-W. Antiproliferation for Breast Cancer Cells by Ethyl Acetate Extract of *Nepenthes thorellii* x (*ventricosa* x *maxima*). *Int. J. Mol. Sci.* **2019**, *20*, 3238. [[CrossRef](#)] [[PubMed](#)]
22. Zhang, X.; Samadi, A.K.; Roby, K.F.; Timmermann, B.; Cohen, M.S. Inhibition of cell growth and induction of apoptosis in ovarian carcinoma cell lines CaOV3 and SKOV3 by natural withanolide Withaferin A. *Gynecol. Oncol.* **2012**, *124*, 606–612. [[CrossRef](#)] [[PubMed](#)]
23. Kessner, D.; Chambers, M.; Burke, R.; Agus, D.; Mallick, P. ProteoWizard: Open source software for rapid proteomics tools development. *Bioinformatics* **2008**, *24*, 2534–2536. [[CrossRef](#)] [[PubMed](#)]
24. Wang, M.; Carver, J.J.; Phelan, V.V.; Sanchez, L.M.; Garg, N.; Peng, Y.; Nguyen, D.D.; Watrous, J.; Kapono, C.A.; Luzzatto-Knaan, T.; et al. Sharing and community curation of mass spectrometry data with Global Natural Products Social Molecular Networking. *Nat. Biotechnol.* **2016**, *34*, 828–837. [[CrossRef](#)] [[PubMed](#)]
25. Shannon, P.; Markiel, A.; Ozier, O.; Baliga, N.S.; Wang, J.T.; Ramage, D.; Amin, N.; Schwikowski, B.; Ideker, T. Cytoscape: A Software Environment for Integrated Models of Biomolecular Interaction Networks. *Genome Res.* **2003**, *13*, 2498–2504. [[CrossRef](#)]